JOURNAL OF BACTERIOLOGY, June 1995, p. 3283–3294
0021-9193/95/$04.00+0

Vol. 177, No. 11

S Gene Expression and the Timing of Lysis by Bacteriophage λ

CHUNG-YU CHANG,[1]† KIEBANG NAM,[1]‡ AND RY YOUNG[1,2]*

Department of Biology[1] and Department of Biochemistry and Biophysics,[2] Texas A&M University, College Station, Texas 77843-2128

Received 20 December 1994/Accepted 20 March 1995

The *S* gene of bacteriophage λ encodes the holin required for release of the *R* endolysin at the onset of phage-induced host lysis. *S* is the promoter-proximal gene on the single λ late transcript and spans 107 codons. *S* has a novel translational initiation region with dual start codons, resulting in the production of two protein products, S105 and S107. Although differing only by the Met-1–Lys-2. . . N-terminal extension present on S107, the two proteins are thought to have opposing functions, with the shorter polypeptide acting as the lysis effector and the longer one acting as an inhibitor. The expression of wild-type and mutant alleles of the holin gene has been assessed quantitatively with respect to the scheduling of lysis. *S* mRNA accumulates during the late gene expression period to a final level of about 170 molecules per cell and is maintained at that level for at least the last 15 min before lysis. Total S protein synthesis, partitioned at about 2:1 in favor of the S105 protein compared with the other product, S107, accumulates to a final level of approximately 4,600 molecules per cell. The kinetics of accumulation of S is consistent with a constant translational rate of less than one S protein per mRNA per minute. Mutant alleles with alterations in the translational initiation region were studied to determine how the translational initiation region of *S* achieves the proper partition of initiation events at the two *S* start codons and how the synthesis of S105 and S107 relates to lysis timing. The results are discussed in terms of a model for the pathway by which the 30S ribosome–fMet-tRNA complex binds to the translational initiation region of *S*. In addition, analysis of the relationship between lysis timing and the levels of the two *S* gene products suggests that S107 inhibits S105, the lethal lysis effector, by a stoichiometric titration.

Evidence has accumulated that lysis is a precisely scheduled event in phage λ infection (10, 19, 37, 42). In the λ genome, the lysis genes *S*, *R*, and *Rz* lie in an overlapping cluster, the first genes downstream of the single late promoter in λ, p'_R (Fig. 1). The *R*, or endolysin, gene encodes a soluble transglycosylase which accumulates intracellularly throughout the late protein synthesis phase of the infective cycle (4, 13). The *Rz* gene has an unknown function and is not required for lysis under laboratory conditions, except when the outer membrane is stabilized with high concentrations of divalent cations (8, 46). The *S* gene encodes a small (M_r = 8,500) inner membrane protein which acts to permeabilize the membrane in some way to allow endolysin access to the periplasm and its substrate, the peptidoglycan (2, 3, 15, 16). The membrane lesion mediated by *S* forms suddenly, late in the infective cycle, with the result that, even in the absence of endolysin, respiration halts, small molecules leak out of the cell, and the cell dies, although it does not lyse (1, 27, 28, 33). The lesions appear to be nonspecific, at least to the extent that they permit the escape of several totally unrelated endolysins from different phages (7, 20, 30, 38). The predicted product of the *S* gene has a distinctive arrangement of hydrophobic, hydrophilic, and charged residues which are shared by the predicted products of genes that are functionally homologous but dissimilar in sequence. The term holin has been coined for this group of lysis proteins (42, 43).

The lambdoid holin genes have an unusual 5′ motif in which there are two start codons separated by one or more positively charged residues (Fig. 1). It has also been demonstrated that both start codons are utilized in vivo, generating two protein products, designated S107 and S105 according to the length of each polypeptide translation product in amino acid residues (5, 10). Dominant lysis-defective mutations have been found upstream of *S* and define the *sdi* stem-loop structure in the RNA (26). These mutations were the first clues suggesting that there was a translational control system which defined the partition of translational initiation events between the two start codons and that the two protein products act antagonistically in lysis timing, with the S107 protein acting to retard the lytic event and S105 acting as a lethal lysis effector. This "dual-start" motif has been found to be evolutionarily conserved in all other lambdoid phage holin genes sequenced to date (42, 43), presumably because it has a substantial effect on lysis timing and thus on the burst size (9).

Using primer extension inhibition ("toeprinting") analysis in a purified system with 30S ribosomes, tRNA, and *S* mRNA, Bläsi et al. (6) studied the effect of site-directed mutations in the 5′ region of the *S* gene on ternary complex formation over the Met-1 and Met-3 start codons. On the basis of the results of these studies, six elements were proposed to control the partition of translational initiation events on the *S* mRNA: the two start codons (Met-1 and Met-3), a near-consensus Shine-Dalgarno sequence (GGGGG from nucleotide [nt] −12 to −7) serving the Met-1 start codon for S107, an unusual Shine-Dalgarno sequence (UAAG from nt −6 to −3) serving the Met-3 start codon for S105, the upstream *sdi* stem-loop structure (spanning nt −21 to −7) which occludes the GGGGG sequence, and a second, intragenic stem-loop (spanning nt +31 to 47) (see Fig. 1). The findings of the toeprint experiments suggested that the two stem-loop structures seemed to play complementary roles in controlling the partition of translational initiation events between the two start codons. That is, strengthening and weakening the downstream stem-loop structure reduced and increased the formation of initiation com-

* Corresponding author. Mailing address: Department of Biochemistry and Biophysics, Texas A&M University, College Station, TX 77843-2128. Phone: (409) 845-2087. Fax: (409) 862-4718. Electronic mail address: YOUNG@BIOCH.TAMU.EDU.

† Present address: Worcester Foundation for Experimental Biology, Shrewsbury, MA 01545.

‡ Present address: Samsung Biomedical Research Institute, Center for Basic Research, Kangnam-Ku, Seoul 135-20, Korea.

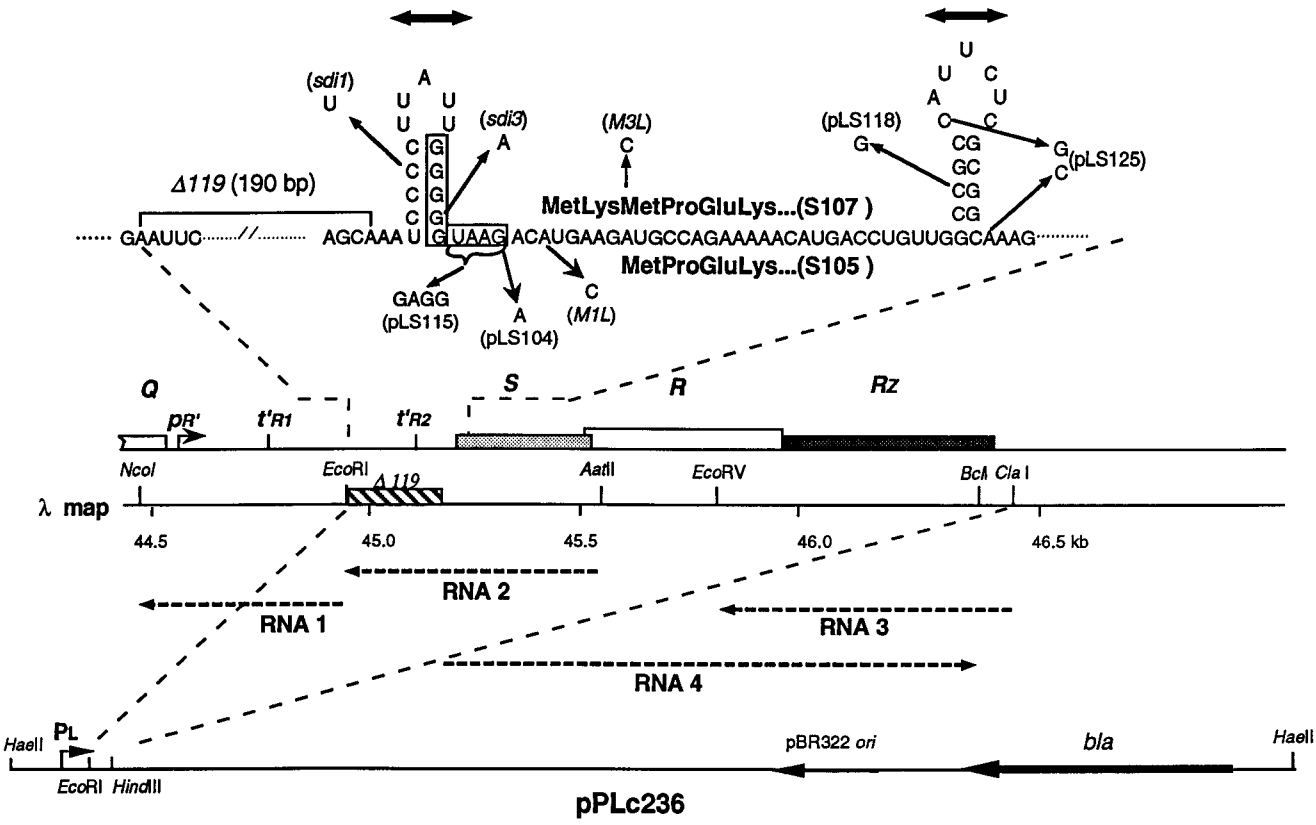

FIG. 1. Structure of the *S* translation initiation region and pLS plasmid series. The sequence of the 5′ region of the *S* mRNA is shown, with the two stem-loop RNA secondary structures previously characterized in vivo and in vitro (6, 23, 26) designated by the thick, double-headed arrows. The upstream structure, defined by the *sdi* mutations (26), spans nt −21 to −8, and the downstream (intragenic) structure spans nt +33 to +47. Arrows indicate sequence changes for various *S* alleles and pLS variants, described previously (6). The N-terminal amino acid sequences of the S107 and S105 proteins are shown above and below the mRNA sequence, respectively. Rectangular boxes surround the Shine-Dalgarno sequences serving the Met-1 and Met-3 initiation codons. Also shown is the deletion Δ*119*, which removes 190 bp upstream of the *sdi* stem-loop structure (10). Below the detailed sequence, the position of the 5′ region of *S* is shown in relation to the λ late promoter, p'_R, and the major (t'_{R1}) and minor (t'_{R2}) late transcription terminators (11, 21, 41), as well as the rest of the lysis gene region. Beneath the λ map, the dashed lines indicate the structures of the RNA probes (RNAs 1, 2, and 3) and internal standard RNA (RNA 4) used in the RNase protection assays for assessing λ late gene transcription. In each case, the arrowhead indicates the 3′ end of the RNA. In the pLS series of plasmids (Table 1), the λ DNA fragment from the *Eco*RI site upstream of *S* to the *Cla*I site immediately downstream of *Rz* is inserted into the *Eco*RI-*Hin*dIII sites of the vector pPLc236 (29), which is shown in linearized form below the λ map.

plexes at Met-3, respectively. In contrast, strengthening the *sdi* structure decreased the formation of initiation complexes at Met-1, whereas weakening this structure had the opposite effect. In addition, weakening either structure reduced the total amount of ribosome binding to the mRNA in vitro, suggesting that the two structures played a role not only in the partition of initiation events between the two start codons but also in the overall capacity of the *S* translational initiation region to support ternary complex formation.

In the phage vegetative cycle, *S* is transcribed as a result of antitermination of the p'_R transcript, which is subject to efficient termination at two terminators upstream of the lysis gene region (Fig. 1) (21, 31, 32). Constitutive transcription proceeds for almost 40 min, during which time there is a significant increase in the gene dosage of *S* as a result of DNA replication. Surprisingly, however, there are no direct measurements of the absolute amounts of λ late mRNA synthesis available. Moreover, no direct assessment of S protein synthesis during the normal vegetative cycle has been possible because, for unknown reasons, the available antibodies, raised against S–β-galactosidase fusion proteins in two different laboratories, recognize the S105 product but not the S107 product (10). Chang et al. (10), using [^{35}S]methionine pulse-labelling in an in vivo T7 RNA polymerase expression system which suppressed host protein synthesis, showed that the two products are synthesized at a constant relative rate, about 2:1 in favor of S105, from the moment of induction to the onset of lysis. However, the expression system used is significantly different from the normal context of the infected cell, and lysis timing in this somewhat artificial system is markedly less precise and defined, presumably because of the metabolic perturbations imposed by the extremely high-level activity of T7 RNA polymerase.

In addition, it must be noted that nothing is known about the nature of the "hole" mediated by the holin proteins. A quantitative assessment of the accumulation of S proteins might help constrain possible models for the macromolecular structure of these membrane lesions. In phage and plasmid contexts, the levels of S protein which accumulate before the triggering of lysis have been estimated to be on the order of 300 to 1,000 molecules per cell on the basis of indirect results with *S*::*lacZ* fusion genes (25) and on yields of S protein purified by immunoaffinity chromatography (48). However, no direct measurement of S protein levels has been published. Here we used quantitative immunoblotting to assess S protein accumulation during the late gene expression phase of the phage vegetative cycle and compared it with the accumulation of *S* mRNA. The more refined estimates of the stoichiometry of lysis protein synthesis during the lytic cycle are discussed in

TABLE 1. Bacterial strains, bacteriophages, and plasmids

Strain, phage, or plasmid	Genotype[a]	Description	Source or reference
Strains			
MC4100	*araD Δlac rpsL flbB deoC ptsF rbsR*		35
pop2135	*end A thi hsdR malT* (*cI857* p_R)::*malPQ*	Host for pLS plasmids with *SRRz* under p_L control	O. Raibaud, Institute Pasteur, Paris
Phages			
λ111	λ *cI857 Sam7*		17
λRG1	λ *b519 b515 b2*::Tn*903 cI857 nin5* S^+	Wild-type *S* allele	19
λA52G	λ *b519 b515 b2*::Tn*903 cI857 nin5* S_{A52G}	Early lysis allele	19
λ372	λ *b519 b515 rex*::Tn*903 cI857 nin5 Sam7*	*Sam7* parental for λ119	45
λ119	λ *b519 b515 rex*::Tn*903 cI857 nin5 Δ119* S^+	Contains deletion of 196 bp upstream of *S* gene	10
Plasmids			
pLS157	S^+	Wild-type *SRRz* under p_L control	6
pLS107	*S* M3L	*S* codon 3 changed: AUG→CUG	6
pLS105	*S* M1L	*S* codon 1 changed: AUG→CUG	6
pLS130	*S* M1,3L	*S* codons 1 and 3 changed: AUG→CUG	6
pLS99	G_{-8}→A (*sdi3*)	Upstream stem-loop (*sdi*) destabilized	6
pLS101	C_{-18}→U (*sdi1*)	Upstream stem-loop (*sdi*) destabilized	6
pLS104	G_{-3}→A	Shine-Dalgarno sequence for codon 3 initiation altered: UAAG→UAAA	6
pLS111	Exchange of (UCCCC nt −21 to −17) and GGGGG (nt −11 to −7)	Stems of *sdi* stem-loop reversed; spacing between Shine-Dalgarno sequence and codon 1 changed from 6 to 18 nt	6
pLS115	UAAG (nt −6 to −3) changed to GAGG	Unusual UAAG Shine-Dalgarno sequence for codon 3 initiator changed to consensus	6
pLS118	C_{33}→G	Downstream stem-loop destabilized	6
pLS123	G_{-3}→A and C_{33}→G	Shine-Dalgarno sequence for codon 3 initiation altered: UAAG→UAAA and downstream stem-loop destabilized	6
pLS124	U_{-21}→C	Upstream stem-loop (*sdi*) stabilized	6
pLS125	C_{36}→G and A_{48}→C	Downstream stem-loop stabilized	6
pTZ009		λ DNA between bp 45173 (boundary of Δ*119*) and bp 45567 (*Aat*II), spanning all of *S* inserted in antisense orientation downstream of P_{T7} in vector pTZ18U; template for probe RNA 2	22
pTZ010		λ DNA between bp 44248 (*Nco*I site in *Q*) and bp 44972 (*Eco*RI) inserted as in pTZ009; template for probe RNA 1	22
pTZ111		λ DNA between bp 45830 (*Eco*RV site in *R*) and bp 46439 (*Cla*I) inserted as in pTZ009; template for probe RNA 3	22
pBS119		λ DNA between bp 45173 (boundary of Δ*119*) and bp 46366 (*Bcl*I site in *Rz*), spanning all of *S* and *R* and most of *Rz*, inserted in sense orientation downstream of P_{T7} in vector pBSM13$^-$; template for probe RNA 4 (internal standard)	22

[a] For plasmids, the *S* genotype is given.

relation to S protein function and regulation. In addition, using an inducible plasmid system, we determined the in vivo accumulations of S105 and S107 for each of the collection of mutant alleles previously characterized for the ability to support ternary complex formation over the two *S* start codons in vitro. These results lead to a refinement of our model for the translational control of the *S* gene and the roles of the two proteins in the timing of lysis.

MATERIALS AND METHODS

Bacterial strains, bacteriophages, and plasmids. The bacterial strains, bacteriophages, and plasmids used in this work are shown in Table 1. The pLS series of plasmids (Fig. 1; Table 1) carry the *SRRz* gene cluster inserted downstream of the λ p_L promoter of the vector PLc236, a derivative of pBR322. Details of their construction are given by Bläsi et al. (6). The pTZ series of plasmids were constructed by inserting the indicated fragments of λ DNA (Table 1) into the vector pTZ19U (Pharmacia), as previously described (10). pBS119 was constructed by inserting the λ DNA between bp 45173 and 46366 into the vector pBSM13$^-$, as previously described (10). The nonsuppressing prototroph MC4100 (35) was used as the host for all prophages. The strain pop2135, carrying the λ *cI857* allele inserted in the *malPQ* locus (O. Raibaud, Pasteur Institute, Paris, France), was used as the host for all of the pLS series of plasmids, as previously described (6). The Δ*119* allele, described previously, in the plasmid pLS119 (10) was recombined onto the phage genome by published procedures (26).

Growth media. All bacterial cultures were grown in standard Luria-Bertani medium, supplemented with ampicillin when appropriate, as previously described (6).

Quantitation of λ late mRNA. Attempts to prepare total RNA from induced S^+ lysogens resulted in poorly reproducible yields, presumably because periplasmic RNase activity is allowed access to the cytoplasm by the action of the holin (24). Thus, the kinetics of late mRNA was studied in an *Sam* lysogen. A λ111 lysogen of MC4100 was aerated at 30°C until the A_{550} was 0.2, induced by aerating at 42°C for 20 min, and then aerated at 37°C. (The brief aeration at 42°C inactivates the *cI857* repressor and causes synchronous initiation of the vegetative cycle throughout the culture. By 10 min after induction, the Q protein has

begun antitermination at the major late terminator and thus allows extension of the constitutive p'_R transcripts into the the lysis genes and the more distal head and tail genes). At varous times after induction, samples (20 ml) were transferred to chilled centrifuge tubes, pelleted in the cold, and resuspended in buffer containing 10 mM KCl, 5 mM $MgCl_2$, and 10 mM Tris HCl (pH 7.3). After freshly prepared lysozyme (Sigma) was added to 300 μg/ml, the suspensions were incubated at room temperature for 10 min and frozen in liquid nitrogen. Samples were thawed at room temperature, sodium dodecyl sulfate (SDS) was added to a final concentration of 1%, and the resultant viscous solutions were incubated at 64°C until clear. Each lysate was brought to 100 mM sodium acetate (pH 5.2), extracted with phenol-chloroform, and precipitated in ethanol. The pellet, containing total cellular RNA, was resuspended in 800 μl of 0.1 mM Na_2EDTA. Each total RNA preparation was supplemented with 6.6 μg of internal standard RNA (see below). Before RNase protection assays were performed, total RNA samples were subjected to digestion with RNase-free DNase I (Promega) to eliminate residual DNA. All RNA samples were checked for degradation and DNA contamination by electrophoresis on 1% agarose gels followed by ethidium bromide staining.

Antisense RNA probes spanning the sequences indicated in Fig. 1 were prepared by linearizing the appropriate templates and transcribing with T7 RNA polymerase in the presence of radioactive nucleotides, using the Riboprobe Gemini System II kit (Promega) according to the instructions of the manufacturer. The antisense *S* probe was prepared from pTZ009 linearized with *Eco*RI, generating a 595-nt runoff transcript. Similarly, an antisense probe for upstream sequences was prepared from pTZ010 linearized with *Nco*I, resulting in a 724-nt runoff transcript. An antisense probe for the *R* gene was transcribed from the plasmid pTZ011, linearized with *Eco*RV. The internal standard RNA was prepared similarly, except no radioactive nucleotides were used and the plasmid template was pBS119 (Table 1). An RNase protection assay kit (Ambion) was used according to the directions of the manufacturer. Briefly, 5.0 μg of total cellular RNA was mixed with 5×10^4 cpm of gel-purified antisense RNA probe (approximately 15 ng) in 20 μl of hybridization buffer {80% [vol/vol] deionized formamide, 40 mM PIPES [piperazine-*N*,*N*′-bis(2-ethanesulfonic acid)] [pH 6.4], 400 mM sodium acetate, and 1.0 mM Na_2EDTA}. These mixtures were denatured for 5 min at 95°C and allowed to hybridize overnight at 42°C. Unhybridized RNA was digested with 0.5 U of RNase A and 10 U of RNase T_1 for 30 min at 37°C. Samples were treated with proteinase K in the presence of 0.5% SDS for 15 min at 37°C. After phenol-chloroform extraction and ethanol precipitation, each pellet was resuspended with loading buffer (80% formamide, 0.1% xylene cyanol, 0.1% bromophenol blue, and 2 mM Na_2EDTA), heated at 95°C for 5 min, and analyzed on a 6% polyacrylamide sequencing gel. Signals were quantitated by direct beta-ray detection in a Betagen Betascope. For each lane in Fig. 2, the radioactivity measured for the band corresponding to the RNA probe protected by the mRNA was normalized to the amount found for the band corresponding to the RNA probe protected by the internal standard (Fig. 1).

Quantitative immunoblotting. To quantitate the S protein made in induced lysogens or inducible clones, inner membrane protein samples were prepared as follows. For samples not previously lysed in vivo, either 5 ml of cells was pelleted and resuspended in 3 ml of FP buffer (0.1 M sodium phosphate [pH 7.0], 0.1 M KCl, 5 mM EDTA, 1 mM dithiothreitol, 1 mM phenylmethylsulfonyl fluoride) before being disrupted in an Aminco French pressure cell at 16,000 lb/in^2 or the same volume of culture was directly sonicated with a Heat Systems-Ultrasonics model W-375 sonicator with a microtip set for a pulsed mode for 3 min at output control setting 3 and a 40% duty cycle. After disruption, membranes were collected by centrifugation at 100,000 × *g* for 1 h before extraction in Eppendorf tubes with ME buffer (10 mM Tris Cl [pH 8.0], 35 mM $MgCl_2$, 1% Triton X-100) at a volume of 1/100 of the original culture volume. After being mixed on a platform shaker for 2 h at 25°C, the extracted samples were centrifuged at 100,000 × *g* for 30 min to pellet the Triton-insoluble material. The membrane extracts were mixed with 2× SDS-polyacrylamide gel electrophoresis (SDS-PAGE) sample buffer, heated at 100°C for 3 min, and analyzed on a Tricine-SDS–16.5% polyacrylamide gel, as previously described (33a). After electrophoresis, Western blotting (immunoblotting) was performed by standard techniques (39). An antibody raised in rabbits against a synthetic C-terminal polypeptide from the S sequence was used as the primary antibody at a dilution of 1:500. The secondary antibody solution (goat anti-rabbit immunoglobulin G conjugated to horseradish peroxidase [Pierce Chemicals]) was used at a 1:500 dilution, and the blot was developed according to the directions of the manufacturer. To ensure linearity, several different amounts of partially purified samples of S protein quantitated by relative Coomassie blue staining were always analyzed on the same gels. The S protein standards were obtained from cells with an S-overproducing plasmid (35a). By using densitometry, Coomassie blue staining of a series of protein standards with known concentrations was compared with the staining of the S protein standards over a more-than-10-fold loading range to establish linearity (not shown), and an average value of optical density units per microgram of standard protein was calculated and used for S. Thus, our calculations of the absolute numbers of S proteins present in our samples used to calibrate the Western blots are based on the assumption that S protein stains with Coomassie blue with an affinity similar to that of the protein standards we used (probably accurate to within twofold) (40). Western blots were photographed, and negatives were scanned on a Molecular Dynamics model 300 A laser densitometer. In parallel, blots were scanned at 300 dpi, and the digitized images were analyzed with the NIH Image (version 1.54) public domain software suite (W. Rasband, National Institutes of Health; wayne@helix.nih.gov). Both analysis techniques gave essentially identical results. For comparison of the S protein levels produced by induction of the pLS series of plasmids, the highest A_{550} obtained with cultures before lysis in vivo was used to normalize the amount of protein sample loaded on the gel. For nonlysing cultures, samples were prepared 1 h after induction, and amounts of A_{550} units equivalent to those of the lysing cultures were applied to the gel. Two sets of membrane preparations were quantitated on two blots. To obtain the average, the two sets of S105 and S107 values were first normalized such that the totals of S105 and S107 in the wild-type samples were the same. (Arbitrary densitometry units are presented in Table 3.)

For calculations of average translation rate per mRNA, we used the following rationale. We found that the *S* mRNA increased approximately linearly for about 15 min from 0 to 175 molecules per cell and then remained constant for about 25 min. Integrating, we deduced that there were about 5,400 molecule · min of mRNA per cell · min during the vegetative period. Here we determined that about 4,600 S protein molecules accumulate per cell during this period, and both forms of S protein are stable, as assessed by labelling studies (5, 10). From this we can deduce that the average translation rate, assuming that all of the *S* mRNA detected by the RNase protection assay participates equally well in translation, is about 4,600/5,400 ≈ 0.85 molecules of S protein per min per *S* mRNA.

TABLE 2. Levels of *S* mRNA after lysogenic induction

Time after induction (min)	*S* mRNA level[a]	No. of molecules/cell
0	0	<5
5	0	<5
10	0.018	19
15	0.04	43
20	0.108	116
30	0.163	175
40	0.165	177
50	0.135	145

[a] Relative to the standard (see text).

RESULTS

Kinetics of *S* mRNA synthesis. The kinetics of accumulation of *S* mRNA was assessed by preparing total cellular RNA from samples of an induced lysogenic culture and quantitating *S* mRNA by an RNase protection assay with an antisense RNA probe (Fig. 1; Table 2). The results (Fig. 2) show that the level of *S* mRNA increases from the onset of late gene expression until about midway through the vegetative cycle, after which it is at a constant level. By spiking each RNA preparation with a known amount of an internal standard and measuring the relative intensity in each band compared with that in the standard, it was possible to deduce that the final level of *S* mRNA was about 175 molecules per cell (see Materials and Methods). Identical results were found for the *R* gene, which is immediately downstream of *S* on the later transcript (Fig. 2). Protection assays with a probe for the RNA sequences upstream of *S* yielded a complex pattern of low-molecular-weight species, most of which exhibited the same kinetics of accumulation as the *S* and *R* sequences. This is consistent with these species being the products of the RNase III processing at sites beyond the t'_{R1} terminator, including a known site at nt 209 (12). One species, with a mobility corresponding to the 6S (193-nt) leader RNA for the late mRNA, is undetectable before 10 min, increases to a maximum level at about 30 min, and then rapidly decreases. The simplest interpretation is that termination of some transcripts continues to occur at the t'_{R1} terminator even later than 20 min after the onset of Q-mediated antitermination. Presumably, the increase in this species over the 10- to 30-min interval after induction reflects the increase in gene dosage resulting from DNA replication. In any case, the level of *S* mRNA sequences increases with kinetics expected for constitutive transcription of the gene with increasing gene dos-

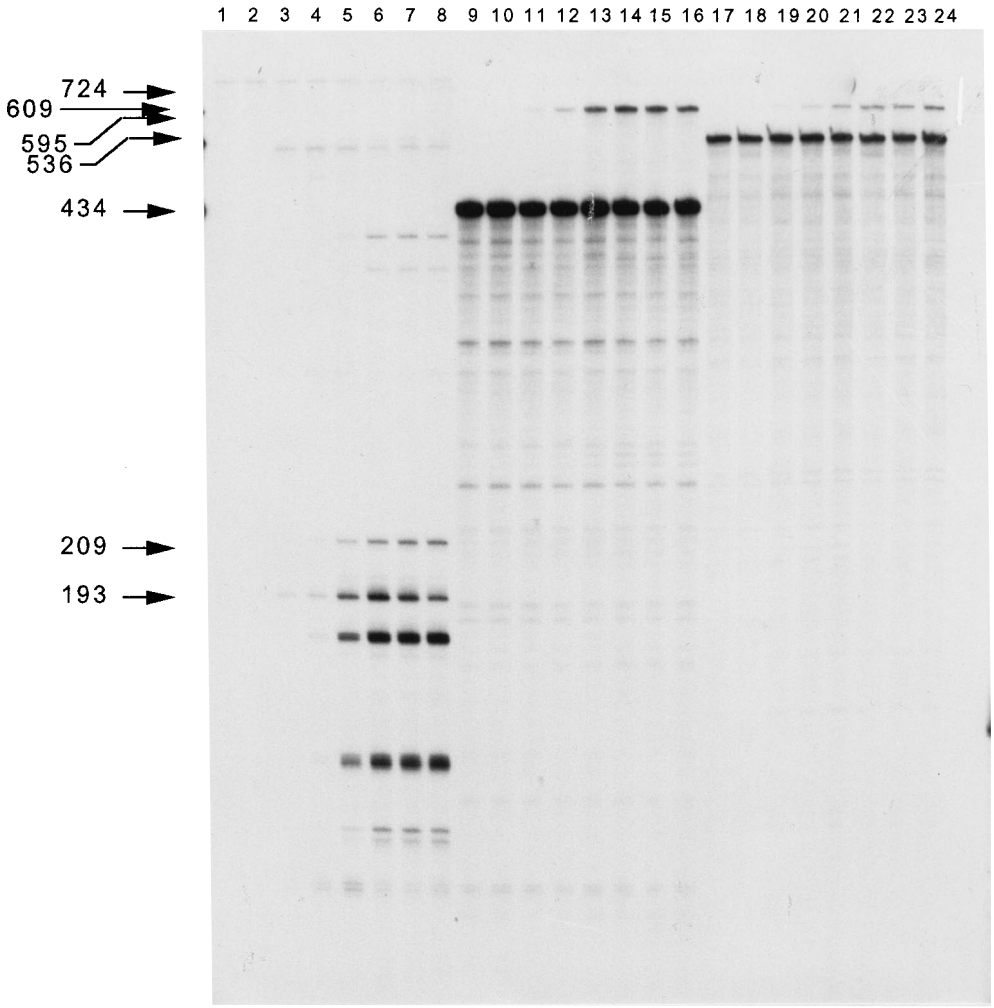

FIG. 2. Accumulation of *S* mRNA after lysogenic induction. RNase protection assays were performed on total cellular RNA at various times after the induction of MC4100(λ111) at $t = 0$ min. Samples were taken at 0, 5, 10, 15, 20, 30, 40, and 50 min after induction, and results are shown in lanes 1 to 8, respectively; lanes 9 to 16, respectively; and lanes 17 to 24, respectively. A constant amount of an internal standard (corresponding to RNA 4 in Fig. 1) was added to each total RNA sample before processing. Antisense RNA probes (Fig. 1) used were RNA 1 (upstream mRNA; lanes 1 to 8), RNA 2 (*S* mRNA; lanes 9 to 16), and RNA 3 (*R* mRNA; lanes 17 to 24). The prominent 434-nt band in the *S* probe lanes (lanes 9 to 16) and the 536-nt band in the *R* probe lanes (lanes 17 to 24) are probe RNAs protected by the internal standard. Other bands are as follows: residual undigested RNA 1 probe (724 nt), *R* probe protected by *R* mRNA (609 nt), *S* probe protected by *S* mRNA (595 nt), major RNase III-processed fragment (209 nt [12]), and 6S RNA (193 nt). Faint bands descending from the protected internal standard bands are minor cleavage products derived from the internal standard.

age up to some time between 20 and 30 min after induction, and there is no evidence for active control of *S* expression at the level of mRNA stability, relative to upstream or downstream mRNA sequences.

Kinetics of S protein accumulation during the λ vegetative cycle. To determine the kinetics of S protein accumulation in the phage vegetative cycle, the ideal experiment would be to use a radioactively labelled amino acid and measure both the rate of synthesis and the net synthesis of S proteins by immunoprecipitation, electrophoretic resolution, and autoradiography. Unfortunately, even with an antibody raised against a polypeptide sequence corresponding to the C terminus of S and thus capable of recognizing each of the two protein products with equal efficiency (10), immunoprecipitation sufficiently clean to allow quantitation of the S bands amidst the contaminating host species could not be achieved (data not shown). However, in immunoblots the anti-C-terminus antibody was found to respond linearly to S protein within an appropriate range of concentrations (not shown), and thus the accumulation kinetics for S protein could be determined by quantitative immunoblotting. Analysis of total membrane samples prepared at various times after induction of a lysogen revealed that total S protein (the sum of S105 and S107) accumulates to approximately 4,600 molecules per cell at the time of lysis (Fig. 3). Moreover, the kinetics of accumulation (Fig. 4) is at least consistent with what would be expected from the pattern of *S* mRNA accumulation (Table 2). In addition, inspection of the immunoblots clearly shows that the proportions of S105 and S107 remain approximately constant all the way up to the onset of lysis (Fig. 3A, lanes 1 to 5 and 9 to 15), in agreement with the results of pulse-labelling experiments conducted with a T7 polymerase-mediated plasmid expression system (10). We conclude, on the basis of the accumulation kinetics of *S* mRNA and S protein after induction, that there is no evidence for active translational control which would alter the total average translational yield or the relative production

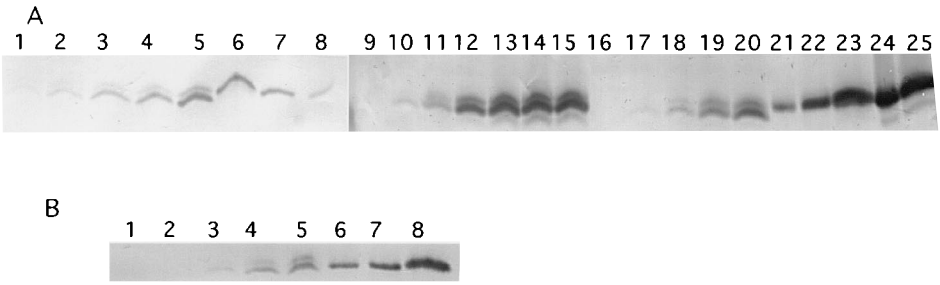

FIG. 3. Accumulation of *S* gene products in induced lysogens. Lysogens carrying the *cI857* thermoinducible repressor and either wild-type or mutant *S* alleles were induced in early logarithmic phase and monitored until lysis was complete. Culture samples were taken at various times and analyzed by membrane protein extraction and Western blotting with an anti-S antibody, as described in Materials and Methods. In each sample from induced cultures, the upper band corresponds to S107 and the lower band corresponds to S105. Standards with known amounts of S107 protein were also analyzed on the same gels. (A) Lanes 1 to 5 and 9 to 15, S^+; lanes 16 to 20, S_{A52G}. Times after induction: 0, 10, 20, 30, and 40 min in lanes 1 to 5, respectively; 0, 5, 10, 20, 30, 40, and 45 min in lanes 9 to 15, respectively; 0, 5, 10, 20, and 25 min in lanes 16 to 20, respectively. S107 protein standards: 3, 6, and 9 pg in lanes 8, 7, and 6, respectively, and in lanes 21 to 23, respectively; 12 and 15 pg in lanes 24 and 25, respectively. The samples in lanes 9 to 15 were loaded and developed to reveal the accumulation of the S proteins at early times after induction and are thus out of the linear range at later times. Thus, the series of samples in lanes 1 to 5 are normalized to the intensities of the standards in lanes 6 to 8, whereas the samples in lanes 9 to 15 and lanes 16 to 20 are normalized to the standards in lanes 21 to 25. (B) Lanes 1 to 5, $S_{\Delta 119}$. Times after induction: 0, 20, 40, 80, and 140 min in lanes 1 to 5, respectively. S107 protein standards: 3, 6, and 9 pg in lanes 6 to 8, respectively.

of the S105 and S107 species during the vegetative cycle. These results support our earlier conclusion that, for any given physiological condition, the scheduling of the lytic event does not require modulation of the expression of the *S* gene at either the transcriptional or translational level or in terms of the relative production of the two S proteins.

Comparison of S protein accumulation in mutants with altered lysis timing. Two *S* alleles which exhibit drastically altered lysis timing without explicit alteration of the dual-start motif are $S_{\Delta 199}$ (10) and S_{A52G} (change of Ala to Gly at codon 52) (19). The former allele has a deletion of the sequences upstream of the *sdi* translational control region (Fig. 1). In the context of a medium-copy-number plasmid vector with the inducible p_L promoter serving for expression of the cloned lysis gene region, lysis occurs 70 min after induction, compared with 20 min for the S^+ allele (10, 22). When this allele is recombined into the normal context of the late gene region of the phage, however, lysis is much more defective, with only a gradual loss of optical density detectable beginning at about 150 min after induction (Fig. 5). In contrast, the A52G allele exhibits extremely early lysis (Fig. 5). Both *S* alleles have plaque-forming defects, with S_{A52G} causing an efficiency of plating of less than 10^{-3} (19) and $S_{\Delta 119}$ supporting the formation of pinpoint plaques at about unit efficiency (data not shown). The kinetics of S protein accumulation was determined for both mutants by quantitative immunoblotting (Fig. 3). The early-lysis allele supports the onset of lysis at about 20 min after induction of the lysogen, at a point when only about 300 S_{A52G} protein molecules are present in the membrane, approximately 10-fold less than in the wild type and with a normal S105/S107 partition (Fig. 3A and 4). This confirms the conclusion based on qualitative data that the A52G allele supports the synthesis of protein with normal stability, accumulation rate, and S105-S107 distribution but has a defect in its intrinsic lysis "clock" (19).

The Δ*119* allele, which has the wild-type S protein sequence and also supports a normal ratio of S105 to S107 (10), triggers

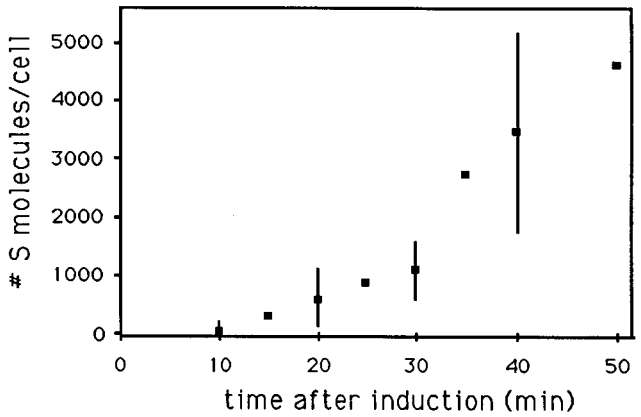

FIG. 4. Kinetics of total S protein accumulation. S protein levels (sum of S105 and S107) determined by quantitative immunoblotting as shown in Fig. 3 and by similar experiments are plotted against the time after induction of the lysogen. The range of one standard error is shown for samples at 10, 20, 30, and 40 min, for results from two experiments. Results for the other samples are from a single experiment. The amount of S is expressed in molecules per induced lysogenic cell. In all cases, lysis onset was observed at about 45 min.

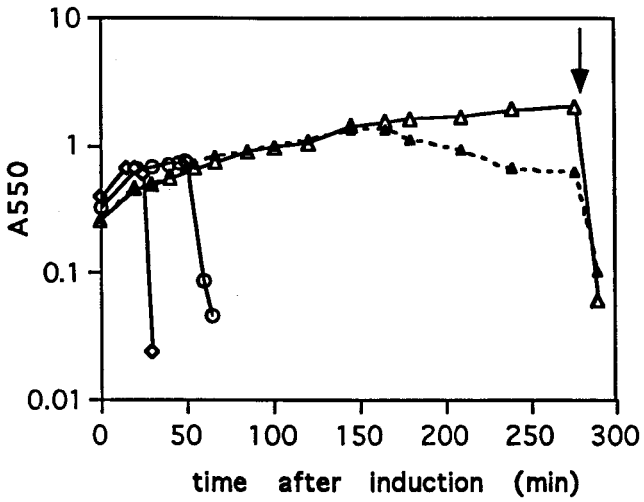

FIG. 5. Lysis kinetics of lysogens with wild-type and mutant *S* alleles. MC4100 lysogens of S^+ (open circles), S_{A52G} (open diamonds), $S_{\Delta 119}$ (closed triangles connected with dashed lines), and *Sam7* (open triangles) were induced in early logarithmic phase, as described in Materials and Methods, and monitored for culture turbidity by A_{550}. At approximately 3 h after induction (arrow), 0.5% $CHCl_3$ was added to release endolysin activity from the unlysed *Sam7* and partially lysed $S_{\Delta 119}$ lysogens.

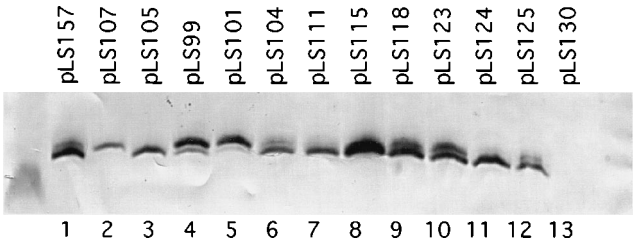

FIG. 6. S105 and S107 production in *S* mutants with altered translational initiation regions. Cells carrying a plasmid from the pLS series (Table 1) with the *SRRz* lysis cassette under p_L control were thermally induced in logarithmic phase. Membrane protein was extracted from the lysed cells, analyzed by SDS-PAGE, and immunoblotted as described in Materials and Methods. A molecular mass marker (5.8 kDa) is visible to the left at lane 1.

lysis, albeit relatively gradually, at about 150 min after induction, when S protein levels have reached approximately 300 molecules per cell (Fig. 3B and 4). In view of the fact that comparable levels of the wild-type protein with the same S105/S107 ratio are reached in the S^+ phage at about 20 min, it is apparent that the timing of lysis onset depends not only on the amount of S protein but also on the rate at which S protein accumulates.

Structural features of *S* mRNA which determine the S105/S107 ratio. With the quantitative immunoblotting approach, we could directly test whether the patterns of ribosome binding in vitro reflect translational initiation in vivo. Using a plasmid system in which the λ lysis gene region is under the expression control of the inducible p_L promoter, we prepared membranes from induced cultures of the entire collection of *S* alleles previously analyzed (6). The results of this analysis are shown in Fig. 6 and quantitated in Table 3 in comparison with the observed pattern of ternary complex formation in vitro. The plasmid pLS157 (Fig. 6, lane 1) carries the wild-type *S* allele and supports the accumulation of S105 and S107 proteins at about a 2:1 ratio, as predicted from the original toeprinting results (6), *lacZ* fusion analysis (5), and the pulse-labelling studies with the T7 expression vectors (10). Comparison of the values obtained for S105 and S107 production with the collection of mutant alleles allows for a number of conclusions which support and refine the model for translational control of *S*.

(i) The *sdi* structure controls access to the Shine-Dalgarno sequence for Met-1. In contrast to the wild-type plasmid, the plasmids pLS99 and pLS101, carrying the negative-dominant *sdi* alleles, predominantly support the synthesis of S107 (Fig. 6, lanes 4 and 5), in general agreement with the in vitro ribosome binding data, at an S107/S105 ratio of 2.7:1 or greater. Thus, the model proposed earlier to explain the negative dominance of the *sdi* alleles appears to be substantiated at the level of protein synthesis; that is, the upstream mutations cause an increase in the proportion of the longer gene product (6, 26). Moreover, two other alleles with alterations in the *sdi* structure which had been found to increase the partition of ternary complexes towards Met-3 at the expense of Met-1 are also found heavily to favor production of S105 protein over S107 (pLS111 and pLS124; Fig. 6, lanes 7 and 11, respectively). In pLS111, this results from a switching of the two arms of the *sdi* structure, such that the GGGGG Shine-Dalgarno sequence is moved too far away from the Met-1 start codon. In pLS124, a U→C mutation adds a G · C base pair to the stem-loop. Presumably, the severe diminution in S107 synthesis arises from stabilization of the *sdi* stem-loop structure. The properties of these four alleles, in comparison with the wild type, strongly support the idea that the role of the *sdi* structure is to occlude the Shine-Dalgarno sequence for Met-1 and thus down-regulate the synthesis of the S107 protein.

(ii) Role of the UAAG sequence. The plasmid pLS104 carries a mutation which alters the UAAG sequence (nt −6 to −3) to the sequence UAAA. The UAAG sequence is complementary to the extreme 3′ end of the 16S rRNA (34). Because the UAAG→UAAA change would eliminate the strongest base pair in this noncanonical interaction, the finding that there was a reduction in the Met-3/Met-1 partition in vitro suggested that the UAAG sequence served as the Shine-Dalgarno sequence, albeit an unusual one, for Met-3 (6, 26). Both in vitro and, as

TABLE 3. S protein levels and lysis time

Plasmid	Description	Level[a]					Time (min)[e]	S107/S105[f]	Met-1/Met-3[g]
		S107	S105	Total S[b]	Normalized total[c]	Excess S105[d]			
pLS115	UAAG→GAGG	0	69.4	69.4	2.21	69.4	10	0.00	0
pLS105	Met-1→Leu	0	15.8	15.8	0.50	15.8	15	0.00	0
pLS124	T-21→C (stabilize *sdi*)	0	31.4	31.4	1.00	31.4	15	0.00	0.24
pLS111	Reverse *sdi* (Shine-Dalgarno sequence for Met-1 removed)	1.4	19.9	21.3	0.67	18.5	18	0.00	0.27
pLS157	Wild type	8.8	22.6	31.4	1.00	13.8	20	0.39	0.42
pLS125	C_{36},A_{48}→G (strengthen downstream stem)	3.3	15.8	19.1	0.61	12.5	25	0.21	0.65
pLS118	C_{33}→G (weaken downstream stem)	21.3	32.2	53.4	1.70	10.9	30	0.66	0.28
pLS104	UAAG→UAAA	4.1	13.7	17.7	0.56	9.6	35	0.30	0.73
pLS123	As for both pLS118 and pLS104	23.2	28.5	51.7	1.65	5.3	50	0.81	0.8
pLS107	Met-3→Leu	8.2	0	8.2	0.26	−8.2	∞		
pLS99	*sdi3*	23.2	4.9	28.1	0.89	−18.3	∞	4.73	2.7
pLS101	*sdi1*	22.1	0.3	22.4	0.71	−21.8	∞	75	2.7

[a] Values for S107 and S105 were determined by densitometry of standardized immunoblots as shown in Fig. 6. Results are for an average of two determinations and are in arbitrary densitometry units (see Materials and Methods).
[b] Sum of the measurements for S105 and S107.
[c] Normalized to the wild-type value.
[d] Arithmetic difference of the measurements for S105 and S107.
[e] Time after induction when the onset of macroscopic lysis is observed (6).
[f] Ratio of the S107 and S105 values.
[g] Ratio of the amount of ternary complex formation over the Met-1 AUG and Met-3 AUG codons, as determined by toeprinting measurements (6).

seen here, in vivo (Fig. 6, lane 8), the replacement of the UAAG sequence with GAGG, a consensus Shine-Dalgarno sequence (plasmid pLS115), causes exclusive utilization of Met-3, which would seem to support the notion that this sequence plays a direct role (as a Shine-Dalgarno sequence) in S105 synthesis. However, in vivo, the pLS104 plasmid supports a wild-type S105/S107 ratio (Fig. 6, lane 6), suggesting that this idea was incorrect. Instead, the ability of a consensus Shine-Dalgarno sequence positioned at the appropriate distance upstream from Met-3 to support increased S105 synthesis may simply reflect that, in the wild-type context, Met-3 does not have a specific Shine-Dalgarno sequence at all (see Discussion).

(iii) Role of the downstream stem-loop structure. In the plasmid pLS118, in which the downstream stem-loop is destabilized by removal of a G · C base pair from the stem, ternary complex formation over Met-3 was found to be increased in vitro, but in vivo the S107/S105 ratio is actually increased (Fig. 6, lane 9). The increase is mostly due to a dramatic increase in S107 (more than twofold), whereas S105 increases only by about 50%. When the same structure is strengthened by addition of a G · C base pair (pLS125), the S107/S105 ratio is decreased, again a change opposite to the prediction based on the pattern of ternary complex formation in vitro. These results suggest that one aspect of the original model, in which the downstream stem-loop acts to control access to the initiation site for translation of the S105 reading frame (6), is not valid.

(iv) Features involved in the total translational efficiency of *S*. In the in vitro studies, the total amount of binding of 30S ribosomes in ternary complexes was assessed. It was found that for alleles in which there were alterations to any of the elements of the *S* translational control region, the total amount of binding was unaffected or marginally affected (e.g., pLS111 and pLS125) or was significantly reduced (e.g., pLS123, pLS104, and pLS118). That is, in no case was the total amount of binding increased over that with the wild-type allele. The in vivo results differ dramatically from these findings. First, in several cases, the total translational output is significantly increased, especially in the plasmid pLS115, in which the consensus Shine-Dalgarno sequence GAGG serves Met-3. Interestingly, the other two alleles for which a significant increase in total S protein production was detected (pLS118 and pLS123) both contain a mutation which destabilizes the downstream loop. Moreover, stabilization of this structure significantly reduces total S synthesis (pLS125; Fig. 6, lane 12). These results imply that the downstream structure is a negative effector for ribosome initiation on the *S* mRNA. It is also worth noting that alterations which eliminate either start codon (pLS105 and pLS107; Fig. 6, lanes 2 and 3, respectively) reduce total S synthesis by about the proportion expected from the S105/S107 ratio of approximately 2:1 for the wild-type allele. In addition, the two changes which eliminate or greatly reduce S107 production without affecting the stability of the *sdi* structure (plasmids pLS111 and pLS105) reduce total S production by about the original amount of S107 synthesis. These data are consistent with the notion that the initiation events at Met-1 are mechanistically downstream of initiations at Met-3. In other words, eliminating the Met-1 pathway without altering the *sdi* secondary structure does not augment the flow of ribosomes to the Met-3 initiation pathway. In any case, for some alleles there is a significant discrepancy between the total ternary complex formation measured in vitro and the total translational efficiency of the *S* mRNA in vivo, as reflected in the amounts of S105 and S107. In general, it appears that the total amount of 30S binding measured in the toeprinting assays is not always a reliable indicator for the ability of the *S* mRNA to support translation in vivo. These data led to modifications of our model for the translational control of the *S* gene (see Discussion).

The relative amounts of production of S105 and S107 determine lysis timing. In Table 3, the collection of mutant alleles of *S* are listed in order of the time required after induction of transcription before the onset of lysis is detectable as a very sharp decrease in the turbidity of the culture (6). When the amounts of the two *S* gene products are considered with respect to these timing data, it is immediately apparent that both the relative and absolute amounts of each protein have a striking impact on the scheduling of lysis. Previous experiments have suggested that the S107 protein acts as an inhibitor of the lytic effect of S105, both when the two proteins are supplied from alternative translational starts on the same mRNA and when they are supplied from separate genes (5, 6, 23, 26). A comparison of the lysis kinetics of the plasmids pLS124, pLS157 (wild type), and pLS123 reinforces this conclusion. Approximately the same amount of the S105 protein is produced in all three, but the delay before the onset of lysis increases with the amount of S107. Moreover, in every case in which the S105/S107 ratio is less than unity, lysis does not occur spontaneously (pLS107, pLS99, and pLS101), whereas whenever S105 is produced in excess of S107, spontaneous lysis does occur (all other alleles except pLS130, with which neither protein is produced). This strongly supports the notion that S107 acts as an inhibitor of S105 and that S105 is the actual lysis effector.

At present, we have no evidence which speaks directly to the mechanism by which S107 can function as an inhibitor of S105, other than the fact that the operative difference between the two molecules is the positively charged residue (Lys-2) at the N terminus of S107 (5, 23, 26). However, some insight can be obtained from considering the quantitative relationships of total S protein and each of the two protein species with lysis time (Table 3). The original analysis based on the toeprinting studies of *S* mRNA suggested that the S107/S105 ratio might be the parameter which determines lysis scheduling (6). However, the availability of the S protein measurements for the same collection of plasmids allows us to reject this notion (compare the S107/S105 ratios for pLS125 and pLS104 with that for pLS157 in Fig. 6 and Table 3). Moreover, neither total S protein production nor even total S105 production correlates well with lysis time (compare pLS157 with pLS118 and pLS123). In fact, when the observed lysis times are plotted versus the total S protein (not shown), the absolute amount of S105 (Fig. 7B), the ratio of S107 to S105 (not shown), and the stoichiometric difference between S105 and S107 (i.e., the excess of S105 over S107) (Fig. 7A), it is striking that a monotonic dependence is exhibited only for the last parameter. That is, lysis time can be considered an inverse function of the excess of S105 over S107 over more than an order of magnitude of this parameter. This result suggests that the inhibitory function of S107 is expressed as a stoichiometric titration of the S105 lysis effector. Moreover, there is apparently a minimum lysis time, approximately 10 min for the standard conditions used in the induction of the pLS series of plasmids. Presumably, beyond a certain point, the excess of S105 over S107 is no longer limiting for the spontaneous triggering of hole formation.

DISCUSSION

Kinetics of *S* gene expression. The data obtained from RNase protection assays of total RNA from induced lysogens indicate that the late gene mRNA levels (for *S* and *R*) increase steadily for the first 15 to 20 min after the onset of late gene

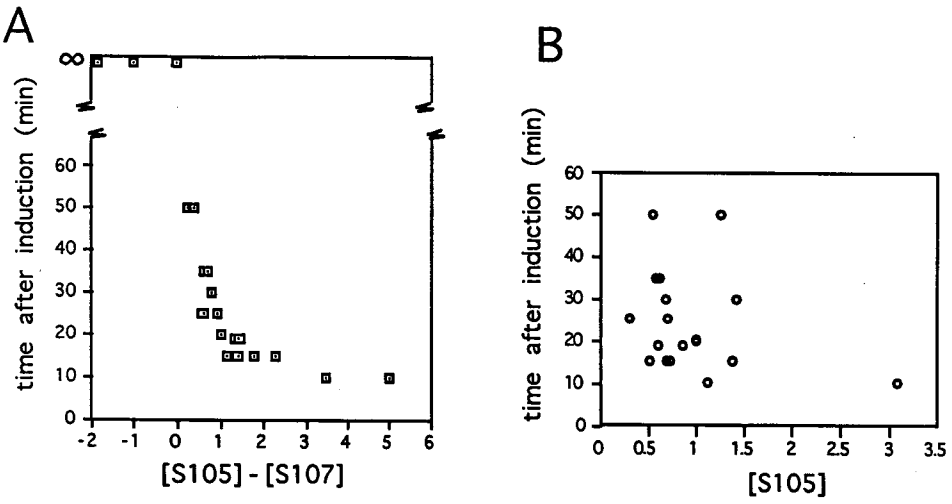

FIG. 7. Dependence of lysis time on S protein levels. The ordinates represent the time required between the beginning of thermal induction and the onset of macroscopic lysis for cultures carrying the various plasmids of the pLS series (see Table 1 and legend to Fig. 6), as determined previously (6). (A) Lysis time plotted against the difference between the S105 and S107 concentrations, as measured from densitometry of quantitative immunoblots such as those shown in Fig. 6. The amount of S105 in excess of S107 in the wild-type clone (pLS157) is set to 1. (B) Lysis time plotted versus the amount of S105. The amount of S105 in the wild-type clone is set to 1.

expression and then remain constant, at about 175 molecules per cell. Assuming a chemical half-life of 2 to 5 min, we can deduce that 25 to 80 mRNA molecules are synthesized per min (44). There are no data concerning the dosage of late genes available for transcription, so we can only estimate the transcriptional activity per genome by making some reasonable assumptions. The normal λ burst is on the order of 100 particles (18). Early in the late gene expression phase, DNA replication has begun to decline and only a small fraction of the total DNA is packaged, suggesting that the available gene dosage might be on the order of 100 molecules. If so, then the average transcription rate per molecule must be quite slow, on the order of 1 per min or less. A low average transcription rate per genome for the *S* and *R* genes may reflect inefficient Q antitermination or a reduction in the transcriptional output of p'_R associated with Q function (30a). In any case, these data allow us to rule out any model in which lysis timing involves regulation at the level of the stability of lysis gene mRNA. In addition, the kinetics of accumulation of the *S* gene products, the S105 and S107 proteins, as assessed by quantitative immunoblotting (Fig. 3), are nicely consistent with the observed kinetics of accumulation of *S* mRNA. These findings indicate that in the phage context, the *S* gene is not under translational control which is manifested in terms of altered translational efficiency or a change in the partition of S105 and S107 production. In other words, the timing of S function, as visualized by the macroscopically visible onset of lysis, is not determined by temporal alterations in the pattern of *S* gene expression. Instead, both S protein products accumulate in the membrane continuously after the onset of late gene expression.

Translational efficiency of the *S* mRNA. The quantitative immunoblotting data of Fig. 3 and 4 reveal that about 4,600 S molecules are produced, with a kinetics consistent with the accumulation pattern of the *S* mRNA. Thus, the production of S protein appears to be at a constant rate of less than 1 molecule of S per mRNA per min, assuming that all of the mRNA molecules detected by the RNase protection assay are equal participants in protein synthesis (see Materials and Methods). Compared with the rate of translation of the well-studied *lacZ* gene, which is translated at a rate of about 30 molecules of β-galactosidase monomers per min (44), this is a very low total translational efficiency. Moreover, deletion of the RNA sequence immediately upstream of the *sdi* stem-loop reduces the total yield at least 10-fold, without affecting the mRNA stability (10). This indicates that the translational initiation region of *S*, severely restricted as it is for productive ribosome binding, apparently requires the presence of upstream RNA structures or protein factor binding sites. These observations underscore the evolutionary pressure to limit expression of the *S* gene and thus effect a lysis program which is consistent with a particle burst of adequate size.

Evaluation of the previous model for S105/S107 partition. The in vitro studies which used toeprinting to measure ternary complex formation over the two *S* start codons in the collection of *S* alleles represented by the pLS series of plasmids led to a model for the pathway by which the 30S ribosome "decide" between initiation at Met-1 and Met-3. Basically, the idea was that the ribosome or ribosome-tRNA complex bound initially to the mRNA sequence between the two stem-loop structures. Subsequently, either the 5′ (*sdi*) structure of the downstream (intragenic) structure would denature, permitting positioning of the loaded P site over the Met-1 or Met-3 start codon, respectively. This model accounted for a number of observations made in the in vitro binding experiments. Most importantly, it explained why weakening either stem-loop structure led to decreased total binding as well as an increase in the relative proportion of complexes formed over one of the start codons. The data presented here, based on direct measurements of S105 and S107 accumulation in vivo, mandate some modification of this model, mainly because the correlation between the total ternary complex formation in vitro and the total production of S protein in vivo is not uniform across the collection of alleles studied. Findings of other groups using the toeprinting method parallel the results presented here. For example, Spedding et al. (36) found no correlation between the toeprint signals and the translational efficiencies of various *rpsD* alleles. Those authors noted that the stability of ternary complexes precludes the measurement of true binding affinities by the toeprinting method and that the kinetics of formation of these complexes in vitro are orders of magnitude slower

than they are in vivo, where initiation factors participate (36). The unreliability of the toeprinting method to give an accurate reflection of the total translational efficiency of each *S* allele also presumably reflects the fact that the conditions for ternary complex formation in vitro do not replicate the intracellular environment, especially with regard to the competition from a multitude of other mRNA species. In contrast, however, the partition of ternary complex formation between the two start codons measured in vitro is generally consistent with the relative production of S105 and S107 in vivo, as shown in Table 3. With the exception of the two alleles with altered stability of the downstream stem-loop, every allele which exhibited a bias toward ternary complex formation over Met-1 (compared with the wild type) also shows an increase in the S107/S105 ratio in vivo. Similarly, alleles showing a decrease in the S107/S105 ratio also exhibited a bias towards 30S binding over Met-3. Thus, the toeprinting method is best suited for determining the position of ternary complex formation and the relative efficiencies of different, mutually exclusive start sites on the same mRNA, where other factors, such as competition from heterologous mRNA, are less relevant.

Revised model for control of the S105/S107 partition. The effects of changing the UAAG sequence (nt −6 to −2; Fig. 1) are especially striking. Replacing this sequence with a consensus GAGG Shine-Dalgarno sequence leads to the exclusive synthesis of S105 at a level significantly increased over the wild-type level. This result suggests that an efficient Shine-Dalgarno sequence spaced appropriately from Met-3 eliminates the initiation pathway which would lead to starts at Met-1. Parallel results were found in the in vitro system, leading to the notion that the UAAG sequence was the Shine-Dalgarno sequence serving Met-3. However, the present data show that weakening the capacity of the nt −6 to −2 sequence to pair with the 3′ terminus of 16S rRNA reduces the synthesis of both S105 and S107 significantly. The simplest interpretation is that there is an interaction of the 30S ribosome with the UAAG sequence and that this interaction occurs before the decision point at which partition between the two start codons is achieved. In Fig. 8, such an interaction is depicted as the primary ribosome-mRNA interactions (Fig. 8A), which then leads to stable initiation complexes over either Met-1 (Fig. 8C) or Met-3 (Fig. 8B).

Another aspect of the previous model, the notion that the downstream stem-loop structure acted reciprocally with the *sdi* structure, is not supported by the in vivo data. That is, strengthening the downstream loop had an effect similar to that of weakening *sdi*, resulting in an increase in the Met-1/Met-3 ratio. Instead, the downstream stem-loop seems to act as a general negative effector for overall translation, with a more pronounced negative effect on S107 production. In the absence of other data, one would have to invoke a steric hindrance model, perhaps in which 30S ribosome binding to the translational start region is partially blocked by the downstream secondary structure, which is, after all, only 28 nt distal to the Met-3 start codon. Alternatively, the downstream stem-loop may participate in a higher-order structure or pseudoknot interaction with the *sdi* structure. It should be noted that the loop of this downstream structure can base pair with the near-consensus Shine-Dalgarno sequence which serves codon 1 in both genes (not shown). In addition, the downstream loop in P22 gene *13* can pair with the Shine-Dalgarno sequence which serves as the start codon for the long-form product ($gp13_{108}$). Alternatively, the downstream stem-loop may act to block elongation, as noted for other mRNAs (3a). However, as noted above, altering the stability of the stem-loop affects S107 production more than S105 production (Table 3, entries for

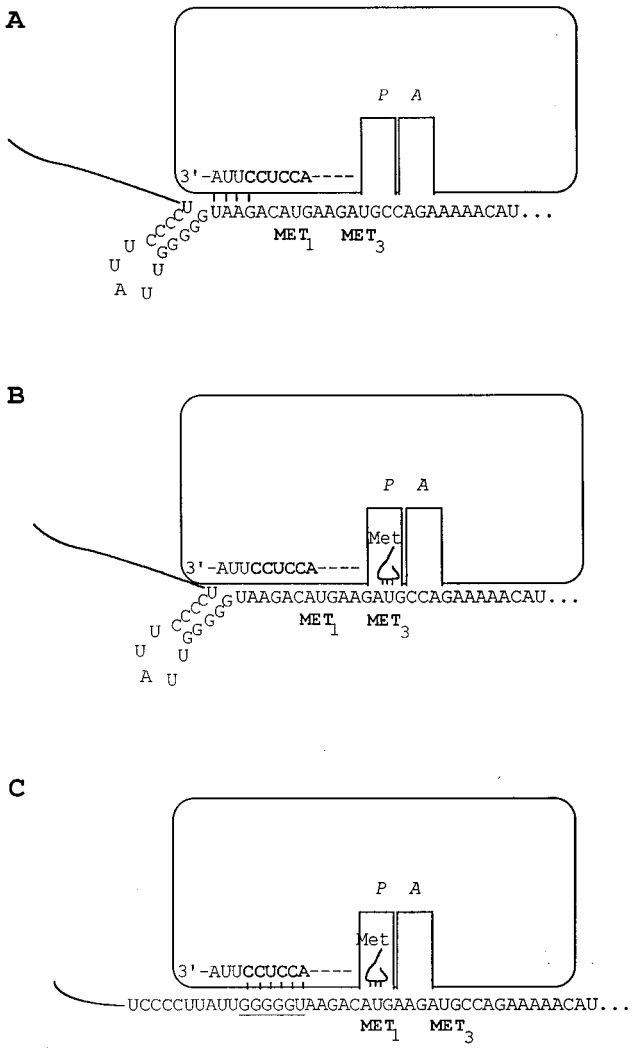

FIG. 8. Model for the partition of initiation events at the two *S* start codons. In each panel, the conserved CCUCC sequence of the 16S rRNA, which pairs with the Shine-Dalgarno sequence in mRNA, is shown at a constant physical distance from the P site of the ribosome. (A) The 30S ribosome–fMet-tRNA complex in a proposed initial binding configuration. In this model, the initial binding is mediated by base-pairing between the extreme 3′ end of the 16S rRNA and the UAAG sequence upstream of the *S* gene. This panel suggests that the 16S rRNA-UAAG interaction leaves the P site out of phase with either AUG start codon. (B) A ternary complex over the Met-3 start codon, the outcome of approximately two-thirds of the initial binding events with the S^+ allele. (C) In about one-third of cases, transient denaturation of the *sdi* stem-loop structure allows formation of the canonical Shine-Dalgarno interaction, resulting in initiation at Met-1 and the synthesis of S107.

pLS157 [wild type], pLS118, and pLS125), and it is not easy to imagine that an elongation block would discriminate between ribosomes which initiate at Met-1 and Met-3.

In the revised model (Fig. 8), initial binding of the 30S particle occurs through interaction of the 16S rRNA with the UAAG sequence. As long as the *sdi* structure remains intact, the ribosome can form productive complexes only over Met-3, which it does at a low rate. Initiations at Met-3 may be impeded by the interaction between UAAG and 16S rRNA, assuming that the physical distance between the CCUCC sequence of the 16S rRNA and the P site is inflexible (Fig. 8). In about one-third of the cases, we presume that there is a transient denaturation of the *sdi* structure and a relocalization of

the 30S ribosome such that the interaction between the canonical Shine-Dalgarno sequence and 16S rRNA occurs (Fig. 8C), leading to initiation at Met-1 and synthesis of S107. Inactivation of the Met-1 start codon (AUG→CUG) has no effect on initiations at Met-3 (Table 3), so presumably complexes which relocate to take advantage of the stronger Shine-Dalgarno sequence but which are frustrated by the absence of the AUG sequences are irretrievably lost. A similar phenotype is associated with alleles carrying mutations which stabilize *sdi* or remove the Shine-Dalgarno sequence to an unfavorable distance from the Met-1 start (Table 3). All essentially cause a fraction of the total *S* translational output to be lost without affecting initiations at Met-3. Loss of the Met-3 AUG reduces overall binding substantially. Thus, although in the M3L mutant (pLS107) (Table 1) the Met-1 codon has no competition, the total amount of S107 production does not increase. Evidently, ribosomes which do not experience the transient denaturing of the *sdi* structure are fated either to dissociate from the mRNA or to initiate at Met-3.

The complex initiation pathway outlined here seems too elaborate to be a consequence only of the primary and secondary structures of the *S* translational initiation region and their interaction with the 30S ribosome. In fact, we have preliminary evidence that a host protein factor binds to this region and participates in the translation initiation pathway (23a). Experiments to identify and characterize this factor are under way and will be described elsewhere. It will be especially interesting to ascertain whether the protein factor responds to environmental signals and affects the S105/S107 ratio and thus the lysis schedule.

Stoichiometry of *S*-mediated lethality. Previous estimates for the stoichiometry of S protein at the time of its lethal action were about 10-fold lower than the estimate of 3,000 molecules per cell determined here. One estimate had been based on the activity of S–β-galactosidase fusions measured at a time after induction when the isogenic *S* plasmid triggered lysis. Presumably, the lower estimates in this case were due to an approximately 10-fold-lower specific activity for the membrane-bound hybrid β-galactosidase. Another estimate was based on the recovery of S protein from an immunoaffinity column, and its low value probably reflects inefficient recognition and binding of S protein in the detergent-solubilized samples. Nothing is known about the distribution of S molecules in the inner membrane. However, inverted membrane vesicles prepared from cells killed by induction of *S* are uniformly leaky (16, 35a). On the order of 10^2 vesicles are derived from each cell, suggesting that membrane lesions may be widespread in the membranes of the killed cells and that no more than 10 to 40 S molecules are required to sustain the lesion. Cross-linking experiments have shown S oligomers up to 8-mers (9, 47, 48) and perhaps higher. Interestingly, the A52G mutant allele, which support extremely early lysis, triggers lysis at a much lower total S protein level, about 10-fold lower than that for the wild-type allele (19), which, according to the quantitation done here, indicates 300 to 600 molecules per cell. As any reasonable model for "holes" in the inner membrane requires high-order S oligomers, one would predict that many of the membrane vesicles prepared from these cells would not be leaky, since the number of S oligomers, even if only 8-mers, would be much lower than the number of vesicles produced.

Scheduling of lysis by S105 and S107. The results presented here provide strong evidence supporting the case that the S105 protein is the effector which is responsible for triggering the spontaneous onset of lysis and that the S107 protein acts to retard lysis by opposing S105 function in some way. Although there are real limitations to the quantitative reliability of comparative immunoblotting, the data summarized in Table 3 and plotted in Fig. 7 indicate that the parameter which best correlates with the timing of lysis is not the total amount of S protein, the amount of S105 protein, or the ratio of the two proteins but instead the stoichiometric difference between the S105 and S107 proteins. The simplest molecular rationale for such a dependence is that S107 titrates out S105 molecules by binding in a 1:1 ratio. This is an attractively simple idea, especially considering the fact that S is known to form multimers in the membrane, and it would be easy to imagine heterodimers formed between S105 and S107, two proteins identical but for two amino-terminal residues in S107. However, immunoprecipitation of S105 from detergent-solubilized membranes has been accomplished with an antibody which does not recognize S107, yet no detectable S107 protein was coprecipitated (10). One possible explanation is that the S105-S107 heterodimers form but do not stably integrate into the membrane, i.e., that the mechanism of the titration is that S107 effectively blocks S105 assembly into the bilayer. This seems unlikely, because S protein detected by labelling or staining has been found only in the membrane fraction (2, 3, 48), but it cannot be ruled out. Alternatively, the S105-S107 complex may not be resistant to nonionic detergent extraction from the membrane. This also seems unlikely, since both S105 and S107 form SDS-resistant homodimers (35a), and it is hard to imagine that the heterodimer could be dramatically less stable and still cause the titration effect. It is not known if these dimers are related to the biological function of either protein or even to the multimeric ladder visualized after chemical cross-linking (48).

At the limit reached in these experiments, the onset of lysis does not occur until at least 10 min after induction, even at the highest level of excess S105. This is consistent with the observation that even with extremely high overexpression of S in a T7 promoter–T7 gene *10* translational fusion mounted on a multicopy plasmid, there is a 15-min lag before *S*-mediated physiological death occurs culture wide (35a). These two lysis times are probably the same, considering that the timing reported here and previously is at 42°C, whereas the T7 expression system is induced at 37°C. These observations suggest that there is a process requiring a rather long macroscopic lag (10 to 15 min) even after S105 protein has accumulated to levels sufficient for lysis triggering. At present, we have no evidence as to what this process might be. One possibility is that some host gene has to be stimulated to function and that the minimum time to lysis simply reflects the phenotypic lag associated with that stimulation. If so, the host gene has resisted genetic identification despite many attempts using powerful selections. Moreover, S functions in yeast cells quite efficiently (14), suggesting that no bacterial host genes are needed for *S*-mediated lethality. In any case, further insight into the remarkable and opposing properties of these two proteins may emerge from in vitro membrane permeabilization experiments currently under way in this laboratory.

ACKNOWLEDGMENTS

We appreciate the assistance and collegiality of the members of the Young laboratory, past and present. Becky Johnson-Boaz's work with the early lysis mutant was crucial background for part of the work reported here. In addition, the helpfulness of the other members of the extended λ and bacteriophage community, including Jeff Roberts, Mark Kainz, Roger Hendrix, and others, is gratefully acknowledged. Udo Bläsi and Karsten Tedin (University of Vienna) were invaluable sources of information, unpublished results, and encouragement over the Internet. Rixin Li and Jim Golden provided essential help in the use of the scanner and of NIH Image software. Some of the photography was done at Biomedical Communications in the Texas A&M University Health Science Center.

This work was supported by Public Health Service grant 27099 to R.Y.

REFERENCES

1. **Adhya, S., A. Sen, and S. Mitra.** 1971. The role of gene *S*, p. 743–746. *In* A. D. Hershey (ed.), The bacteriophage lambda. Cold Spring Harbor Laboratory, Cold Spring Harbor, N.Y.
2. **Altman, E., R. Altman, J. Garrett, R. Grimaila, and R. Young.** 1983. *S* gene product: identification and membrane localization of a lysis control protein. J. Bacteriol. **155:**1130–1137.
3. **Altman, E., K. Young, J. Garrett, R. Altman, and R. Young.** 1985. Subcellular localization of lethal lysis proteins of bacteriophages lambda and ϕX174. J. Virol. **53:**1008–1011.

3a. **Atkins, J. F., R. B. Weiss, and R. Gesteland.** 1990. Ribosome gymnastics—degree of difficulty 9.5, style 10.0. Cell **62:**413–423.

4. **Bienkowska-Szewczyk, K., B. Lipinska, and A. Taylor.** 1981. The *R* gene product of bacteriophage lambda is the murein transglycosylase. Mol. Gen. Genet. **184:**111–114.
5. **Bläsi, U., C.-Y. Chang, M. T. Zagotta, K. Nam, and R. Young.** 1990. The lethal lambda *S* gene encodes its own inhibitor. EMBO J. **9:**981–989.
6. **Bläsi, U., K. Nam, D. Hartz, L. Gold, and R. Young.** 1989. Dual translational initiation sites control function of the lambda *S* gene. EMBO J. **8:**3501–3510.
7. **Bonovich, M. T., and R. Young.** 1991. Dual start motif in two lambdoid *S* genes unrelated to λ *S*. J. Bacteriol. **173:**2897–2905.
8. **Casjens, S., K. Eppler, R. Parr, and A. R. Poteete.** 1989. Nucleotide sequence of the bacteriophage P22 gene *19* to *3* region: identification of a new gene required for lysis. Virology **171:**588–598.
9. **Chang, C.-Y.** 1994. Synthesis, function and regulation of the lambda holin. Ph.D. thesis. Texas A&M University, College Station.
10. **Chang, C.-Y., K. Nam, U. Bläsi, and R. Young.** 1993. Synthesis of two bacteriophage lambda S proteins in an *in vivo* system. Gene **133:**9–16.

10a. **Chang, C.-Y., and R. Young.** Unpublished results.

11. **Daniels, D. L., and F. R. Blattner.** 1982. The nucleotide sequence of the *Q* gene and the *Q* to *S* intergenic region of bacteriophage lambda. Virology **117:**81–92.
12. **Daniels, D. L., M. N. Subbarao, F. R. Blattner, and H. A. Lozeron.** 1988. Q-mediated late gene transcription of bacteriophage lambda: RNA start point and RNase III processing sites *in vivo*. Virology **167:**568–577.
13. **Del Campillo-Campbell, A., and A. Campbell.** 1965. Endolysin from mutants of bacteriophage lambda. Biochem. Z. **342:**485–491.
14. **Garrett, J., C. Bruno, and R. Young.** 1990. Lysis protein S of phage lambda functions in *Saccharomyces cerevisiae*. J. Bacteriol. **172:**7275–7277.
15. **Garrett, J., R. Fusselman, J. Hise, L. Chiou, D. Smith-Grillo, R. Schulz, and R. Young.** 1981. Cell lysis by induction of cloned lambda lysis genes. Mol. Gen. Genet. **182:**326–331.
16. **Garrett, J., and R. Young.** 1982. Lethal action of bacteriophage lambda *S* gene. J. Virol. **44:**886–892.
17. **Goldberg, A. R., and M. Howe.** 1969. New mutations in the *S* cistron of bacteriophage lambda affecting host cell lysis. Virology **38:**200–202.
18. **Hershey, A. D., and W. Dove.** 1971. Introduction to lambda, p. 3–11. *In* A. D. Hershey (ed.), The bacteriophage lambda. Cold Spring Harbor Laboratory, Cold Spring Harbor, N.Y.
19. **Johnson-Boaz, R., C.-Y. Chang, and R. Young.** 1994. A dominant mutation in the bacteriophage lambda *S* gene causes premature lysis and an absolute defective plating phenotype. Mol. Microbiol. **13:**495–504.
20. **Lu, M.-J., and U. Henning.** 1992. Lysis protein T of bacteriophage T4. Mol. Gen. Genet. **235:**253–258.
21. **Luk, K.-C., and W. Szybalski.** 1983. Tandem transcription-termination sites in the late rightward operon of bacteriophage lambda. Mol. Gen. Genet. **189:**289–297.
22. **Nam, K.** 1991. Translational regulation of the *S* gene of bacteriophage lambda. Ph.D. thesis. Texas A&M University, College Station.
23. **Nam, K., U. Bläsi, M. T. Zagotta, and R. Young.** 1990. Conservation of a dual-start motif in P22 lysis gene regulation. J. Bacteriol. **172:**204–211.

23a. **Nam, K., K. Tedin, U. Bläsi, and R. Young.** Unpublished results.

24. **Ono, T., and Y. Ohnishi.** 1981. Degradation of ribosomal RNA in bacteriophage lambda lysogens after thermal induction. Microbiol. Immunol. **25:**433–444.
25. **Raab, R.** 1988. The structure, function and regulation of the *S* gene of bacteriophage lambda. Ph.D. thesis. Texas A&M University, College Station.
26. **Raab, R., G. Neal, C. Sohaskey, J. Smith, and R. Young.** 1988. Dominance in lambda *S* mutations and evidence for translational control. J. Mol. Biol. **199:**95–105.
27. **Reader, R. W., and L. Siminovitch.** 1971. Lysis defective mutants of bacteriophage lambda: genetics and physiology of *S* cistron mutants. Virology **43:**607–622.
28. **Reader, R. W., and L. Siminovitch.** 1971. Lysis defective mutants of bacteriophage lambda: on the role of the *S* function in lysis. Virology **43:**623–637.
29. **Remaut, E., P. Stanssens, and W. Fiers.** 1981. Plasmid vectors for high-efficiency expression controlled by the P_L promoter of coliphage lambda. Gene **15:**81–93.
30. **Rennell, D., and A. R. Poteete.** 1985. Phage P22 lysis genes: nucleotide sequences and functional relationships with T4 and lambda genes. Virology **143:**280–289.

30a. **Roberts, J.** Personal communication.

31. **Roberts, J. W.** 1975. Transcription termination and late control in phage lambda. Proc. Natl. Acad. Sci. USA **72:**3300–3304.
32. **Roberts, J. W.** 1993. RNA and protein elements of *E. coli* and lambda transcription antitermination complexes. Cell **72:**653–655.
33. **Rolfe, B. G., and J. H. Campbell.** 1977. Genetic and physiological control of host cell lysis by bacteriophage lambda. J. Virol. **23:**626–636.

33a. **Schägger, H., and G. von Jagow.** 1987. Tricine-sodium dodecyl sulfate-polyacrylamide gel electrophoresis for the separation of proteins in the range from 1 to 100 kDa. Anal. Biochem. **166:**368–379.

34. **Shine, J., and L. Dalgarno.** 1974. The 3′-terminal sequence of *Escherichia coli* 16S ribosomal RNA: complementary to nonsense triplets and ribosome binding sites. Proc. Natl. Acad. Sci. USA **71:**1342–1346.
35. **Silhavy, T. J., M. L. Berman, and L. W. Enquist.** 1984. Bacterial strains, p. xi–xiii. *In* T. J. Silhavy, M. L. Berman, and L. W. Enquist (ed.), Experiments with gene fusions. Cold Spring Harbor Laboratory, Cold Spring Harbor, N.Y.

35a. **Smith, D., C.-Y. Chang, and R. Young.** Unpublished results.

36. **Spedding, G., T. C. Gluick, and D. E. Draper.** 1993. Ribosome initiation complex formation with the pseudoknotted α operon messenger RNA. J. Mol. Biol. **229:**609–622.
37. **Steiner, M., and U. Bläsi.** 1993. Charged amino-terminal amino acids affect the lethal capacity of lambda lysis proteins S107 and S105. Mol. Microbiol. **8:**525–533.
38. **Steiner, M., W. Lubitz, and U. Bläsi.** 1993. The missing link in phage lysis of gram-positive bacteria: gene *14* of *Bacillus subtilis* phage ϕ29 encodes the functional homolog of lambda S protein. J. Bacteriol. **175:**1038–1042.
39. **Towbin, H., T. Staehelin, and J. Gordon.** 1979. Electrophoretic transfer of proteins from polyacrylamide gels to nitrocellulose sheets: procedure and some applications. Proc. Natl. Acad. Sci. USA **76:**4350–4354.
40. **Winterbourne, D. J.** 1993. Chemical assays for proteins, p. 197–202. *In* J. M. Graham and J. A. Higgins (ed.), Methods in molecular biology, vol. 19. Biomembrane protocols. 1. Isolation and analysis. Humana Press Inc., Totowa, N.J.
41. **Yang, X., J. A. Goliger, and J. W. Roberts.** 1989. Specificity and mechanism of antitermination by Q proteins of bacteriophages lambda and 82. J. Mol. Biol. **210:**453–460.
42. **Young, R.** 1992. Bacteriophage lysis: mechanism and regulation. Microbiol. Rev. **56:**430–481.
43. **Young, R., and U. Bläsi.** Strategies of bacterial lysis. FEMS Microbiol. Rev., in press.
44. **Young, R., and H. Bremer.** 1975. Analysis of enzyme induction in bacteria. Biochem. J. **152:**243–254.
45. **Young, R., and D. Smith-Grillo.** 1980. Transposition of the kanamycin-resistance transposon Tn*903*. Mol. Gen. Genet. **178:**681–689.
46. **Young, R., S. Way, J. Yin, and M. Syvanen.** 1979. Transposition mutagenesis of bacteriophage lambda: a new gene affecting cell lysis. J. Mol. Biol. **132:**307–322.
47. **Zagotta, M. T.** 1989. Characterization of the lambda S protein using antibodies. Ph.D. thesis. Cornell University, Hamilton, N.Y.
48. **Zagotta, M. T., and D. B. Wilson.** 1990. Oligomerization of the bacteriophage lambda *S* protein in the inner membrane of *Escherichia coli*. J. Bacteriol. **172:**912–921.